# Rho overexpression leads to mitosis-associated detachment of cells from epithelial sheets: A link to the mechanism of cancer dissemination

J. M. Vasiliev*†, T. Omelchenko‡§, I. M. Gelfand¶, H. H. Feder§, and E. M. Bonder‡§‖

*Belozersky Institute of Physico-Chemical Biology, Moscow State University, Moscow 119899, Russia; †Oncological Scientific Center of Russia, Moscow 115478, Russia; ‡Program in Cellular and Molecular Biodynamics and §Department of Biological Sciences, Rutgers, The State University of New Jersey, Newark, NJ 07102; and ¶Department of Mathematics, Rutgers, The State University of New Jersey, Piscataway, NJ 08854

Contributed by I. M. Gelfand, July 1, 2004

**Dissemination of neoplastic cells from the primary tumor (invasion and metastasis) is a fundamentally dangerous step in multistage carcinogenesis. Recent evidence suggests that Rho GTPase-mediated signaling is linked to dissemination of cells from several different types of human tumors. The Rho family of proteins is typically associated with the regulation of cytoskeletal activity, including actin assembly, microtubule dynamics, and myosin II-dependent contractility of the actin-rich cortex. We examined the effect of overexpression of constitutively active RhoA on islands and monolayers of epithelial cells. Although newly plated cells initially formed small spread islands, there was also a significant population of cells that detached from the substrate, floated in the medium, and then could reattach to the substrate to form new colonies. Detachment of cells from transfected epithelial islands or monolayers occurred in correlation to the plane of cytokinesis after misorientation of the mitotic spindle axis. We suggest that these alterations result from Rho-induced increase of contractility of the cortex of dividing cells, which, during cytokinesis, produces a cell that has budded out of an existing layer of cells. Cell division-mediated detachment of cells from tissue structures may be an important mechanism of tumor dissemination and metastasis.**

mitotic spindle | metastasis | contractility

The Rho family of small GTPases, Rho, Rac, and Cdc42, plays essential roles in regulating diverse cellular functions, in particular those associated with cytoskeletal dynamics (1–4). Recently, it has been reported that abnormal expression of these proteins may play a fundamentally important role in the molecular mechanisms involved in carcinogenesis (5, 6). Specifically, increased activity and/or expression of the closely related genes *RhoA* and *RhoC* were found in human neoplasms and were further correlated with the degree of malignancy (7–13). As reported by Clark *et al.* (10), overexpression of RhoC enhanced metastasis of mouse melanoma, whereas expression of the dominant-negative Rho variant inhibited metastasis. The mechanism that links Rho activity to the ability of cells within a tumor to spread remains a matter of speculation, since Rho activity potentially impinges on multiple signaling pathways.

To investigate the mechanisms that might link Rho signaling with tumor proliferation, an IAR-2 epithelial cell line expressing constitutively active RhoA was produced by stable transfection with an enhanced GFP (EGFP)-RhoA Q63L plasmid (4, 14). Overexpression of constitutively active RhoA protein produced dramatic changes in cultures of epithelial cells, including overall cell contraction, mass detachment of cells from the monolayer, multilayering of cells creating cell stacking, and subsequent reattachment of stacked cells to the substrate forming new colonies. Detachment of cells is correlated with cell division and is related to improper orientation of the mitotic spindle, which leads to an altered plane for cytokinesis. We propose that this sequence of changes can be considered a culture cell model of a special type of cancer cell dissemination induced by a change in activity of a single gene.

## Materials and Methods

**Cell Culture, Stable Cell Lines, and Drug Treatment.** IAR-2 rat liver epithelial cells (15) and IAR-2 cells stably expressing EGFP-RhoA Q63L (4) were cultured at 37°C in 5% $CO_2$ using DMEM supplemented with 10% FCS (Atlanta Biologicals, Norcross, GA) and antibiotics. The plasmid pEGFP was obtained by excising the tubulin gene from EGFP-Tub (Clontech). A stable cell line expressing EGFP was obtained as described (4). To block cells in S phase of the cell cycle, IAR-2 cells were incubated for 24–48 h in culture media containing 0.5 mM hydroxyurea (Sigma). To inhibit Rho kinase, cells were treated with 15 $\mu$M Y-27632 (Calbiochem).

**Time-Lapse Video Observations.** For video microscopy, cells were grown in glass-bottom chambers (MatTek, Ashland, MA) for 3–5 days. Phase-contrast video microscopy was carried out on a Zeiss Axiovert 200 M microscope by using a ×10 objective lens (numerical aperture 0.55) and a temperature- and $CO_2$-controlled stage. Images were collected at 1- to 5-min time intervals between frames for 2–24 h by using a Zeiss AxioCam camera controlled by AXIOVISION 4 software (Zeiss) and processed by METAMORPH (Universal Imaging, West Chester, PA). To estimate the average area of individual cells, the area of cell islands was measured and divided by the number of cells within the island that are attached to the substrate. Area analysis was performed by using METAMORPH.

**RhoA Pull-down Assay.** To verify activity of the expressed EGFP-RhoA Q63L construct in stably transfected cells, Rhotekin (Rhotek-PBD, Rhotekin protein-binding domain) was used to affinity-precipitate EGFP-RhoA Q63L (16). Rhotek-PBD binds only to the activated GTP-bound form of RhoA. The plasmid pGEX2T-GST-Rhotek PBD was kindly provided by G. Bokoch (The Scripps Research Institute, La Jolla, CA). Expression in *Escherichia coli* BL21 and purification of fusion proteins (GST-Rhotek-PBD and GST) were as described by Benard and Bokoch (17). Affinity precipitation was performed as described by Ren *et al.* (16). Briefly, cells were lysed, sonicated, and centrifuged to obtain cell lysates. Cell lysates (500 $\mu$l) were incubated with GST-Rhotek-PBD-bound beads (30 $\mu$g) for 30 min at 4°C, and then the beads were washed by repeated sedimentation followed by analysis on 7.5–15% SDS/PAGE. The resolved proteins were transferred to nitrocellulose and probed with mouse monoclonal anti-GFP antibody (JL-8) (BD

Abbreviation: EGFP, enhanced GFP.

‖To whom correspondence should be addressed. E-mail: ebonder@andromeda.rutgers.edu.

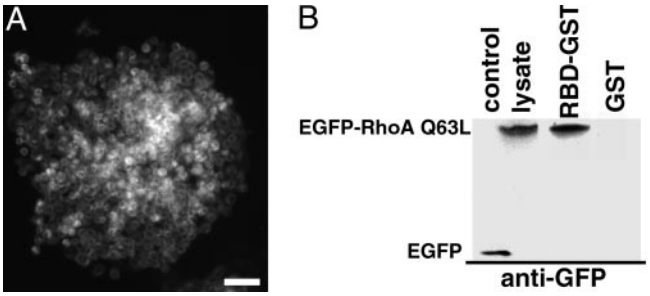


**Fig. 1.** IAR-2 epitheliocytes stably express functional constitutively active RhoA (EGEP-RhoA Q63L) protein. RhoA expression was confirmed by fluorescence in live cells (*A*) and by immunoblotting total cell proteins (*B*). (*A*) An island of cloned IAR-2 epithelial cells stably expressing EGFP-RhoA Q63L. This same island of cells is shown by phase-contrast microscopy in Fig. 2*C*. (Bar = 50 $\mu$m.) (*B*) RhoA pull-down assay examining activity of RhoA construct. Transferred cells were lysed, and EGFP-RhoA Q63L was affinity precipitated by using recombinant GST-Rhotek-PBD (RBD-GST) bound to latex beads. EGFP-RhoA Q63L bound to RBD-GST and the expression of EGFP-RhoA Q63L were analyzed by Western blotting with anti-GFP antibodies. IAR-2 cell stably expressed EGFP (control) or EGFP-RhoA Q63L (lysate). EGFP-RhoA Q63L was bound to GST-RBD (RBD-GST), indicating the expressed construct was functionally active. EGFP-RhoA Q63L did not bind to GST beads (GST).

Biosciences, Clontech; dilution 1:1,000). Blots were incubated with alkaline phosphatase-conjugated secondary antibodies (Zymed) and 5-bromo-4-chloro-3-idolyl phosphate/nitro blue tetrazolium (Sigma) as a chromogenic substrate.

**Cell Count and Viability Assay.** To determine viability and number of detached cells, cultures were incubated for 3–4 days in 25-cm$^2$ flasks. The medium (5 ml) was aspirated, and 200 $\mu$l of aliquot was taken ("detached cell" sample). Spread cells in the same flask were detached in 2 ml of fresh medium, and 200 $\mu$l of aliquot was taken ("attached cell" sample). A standard cell count procedure was performed on both samples by using a hemocytometer and staining with 0.4% trypan blue (Sigma).

**Immunofluorescence Microscopy.** Cells were washed in PBS, fixed in −20°C methanol for 10 min, and stained for microtubules with mouse antitubulin antibody IgG1 clone DM1$\alpha$ (Sigma; 1:50 dilution) or for E-cadherin with mouse anti-E-cadherin IgG1 (BD Biosciences, Pharmingen; 1:50 dilution). All primary antibodies were detected by using anti-mouse Alexa Fluor 488-conjugated secondary IgG antibodies (Molecular Probes; 1:200 dilution). To observe chromosomes, cells were stained with propidium iodide (BD Biosciences, Pharmingen; 1:5 dilution). For actin filament staining, cells were fixed in 3.7% formaldehyde and incubated with rhodamine–phalloidin (Molecular Probes; 1:50 dilution). Confocal images were taken by using the Bio-Rad MRC 1024 laser-scanning confocal microscope system. Stacks of confocal *x-y* images were taken with 0.5-$\mu$m step size, and *x–z* projections were reconstructed by using Bio-Rad LASERSHARP 2000 software.

## Results

To investigate the effect of RhoA activity on the phenotype of monolayers of epithelial cells, IAR-2 cells were stably transfected with the constitutively active RhoA construct, EGFP-RhoA Q63L. After selection and subcloning, >95% of the cells in these cultures expressed readily detectable RhoA protein as manifested by green fluorescence in the cytoplasm (Fig. 1*A*). Activity of the overexpressed EGFP-RhoA Q63L construct was confirmed by using a RhoA pull-down assay. The EGFP-RhoA Q63L construct was constitutively active, as evidenced by its binding to Rhotek-PBD-linked beads (Fig. 1*B*; also see ref. 16).

Nontransfected IAR-2 rat liver epithelial cells (15) form regular islands and sheets of monolayers (Fig. 2*A*) and sheets that contain circumferential bundles of actin filaments associated with E-cadherin-containing cell–cell contacts (18). In monolayers, individual cells have actin bundles and stress fibers with paxillin-positive focal contacts at their ends as well as networks of microtubules (3). In contrast to control cells, cultures of transfected cells were multitiered, with the lower layer consisting of spread cells attached to the substrate and upper tiers of nearly spherical cells (Fig. 2 *B–D* and Movies 1 and 2, which are published as supporting information on the PNAS web site). The majority of the cells attached to the substrate appeared spread and retained the basic shape of control nontransfected cells. In addition to multitiering, another morphological difference was a dramatic decrease in surface area in cells expressing constitutively active RhoA. The surface area of nontransfected cells was approximately twice (415 ± 70 $\mu$m$^2$; ±SEM; $n$ = 170) as large as the surface area of transfected cells (176 ± 18 $\mu$m$^2$; ±SEM; $n$ = 130), suggesting the presence of an overall cellular contraction. The spherical cells located in the upper tier appeared loosely associated with the lower adherent cells, and they often formed small masses of 2–20 cells (Fig. 2 *B–D*).

Rho kinase is one of the main targets of RhoA activation, which leads to stimulation of myosin II-dependent contractility (19). To test whether the observed changes in cell morphology were a consequence of stimulating myosin II contractile activity,

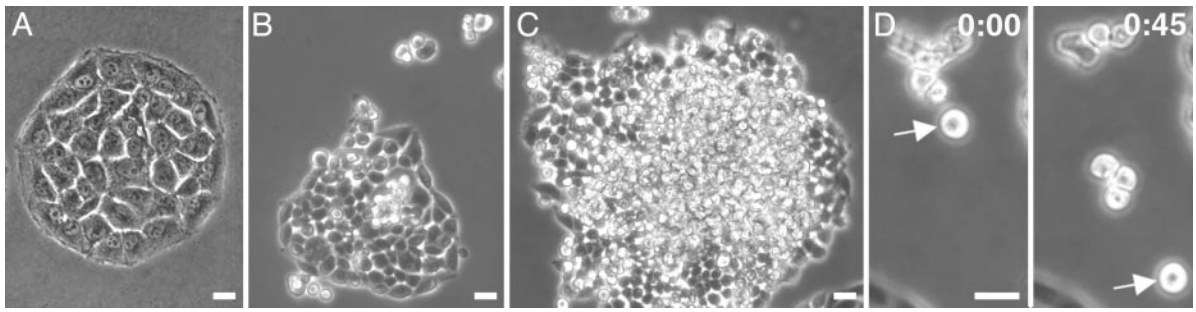


**Fig. 2.** Stable expression of constitutively active RhoA in IAR-2 epitheliocytes leads to cell rounding, multitiering of cells, and detachment of spherical cells from islands. (*A*) Phase-contrast micrograph shows monolayer island of control culture of nontransfected IAR-2 epithelial cells. (*B*) Cultures stably transfected with EGFP-RhoA Q63L (*B–D*) formed colonies of irregular shape and started to develop multiple tiers of cells (shown after 3 days of incubation). The overall size of transfected cells was reduced significantly, and cells attached to the substrate were reasonably spread, whereas cells in the upper tier were spherical. (*C*) After longer incubation times (5 days), the epithelial island consisted of spread lower cells and a dramatically increased number of round highly refractile cells tiered on the substrate attached cells. See Movie 1 for dynamics of these round cells. (*D*) Two frames taken from a time-lapse video (see Movie 2) show a group of round cells that detached from one another and that proceeded to move along the surface of the substrate. Arrow shows the same cell at time 0 and 45 min later. (Bar = 20 $\mu$m.)

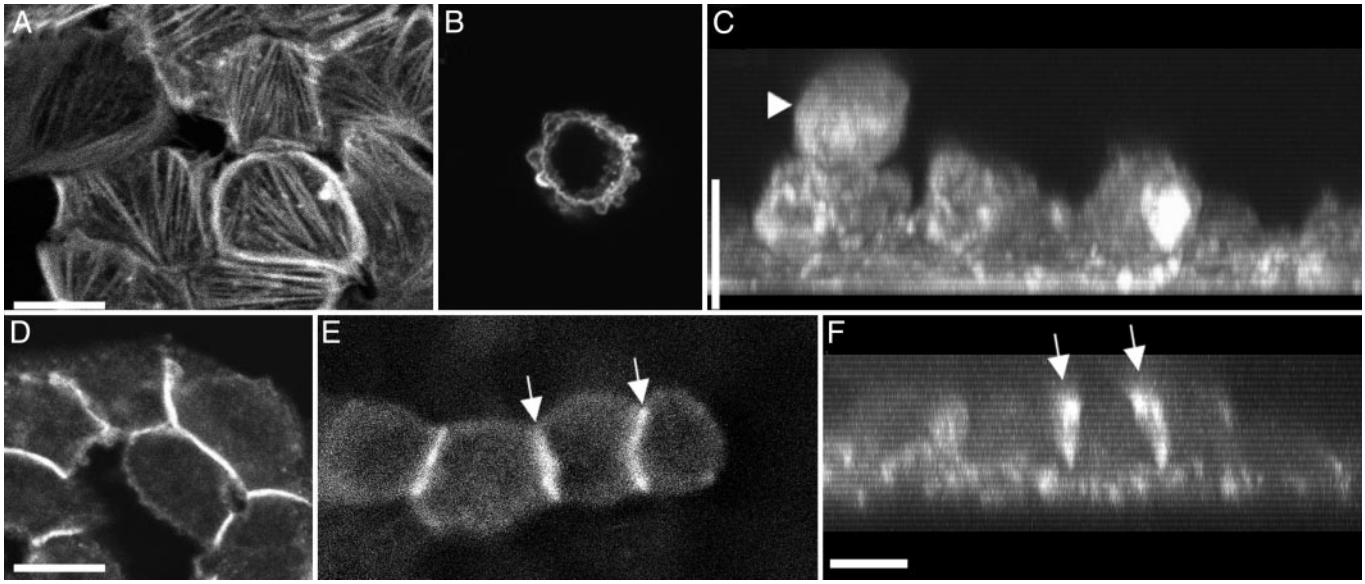


**Fig. 3.** Localization of actin filaments and cell–cell contacts in transfected IAR-2 epitheliocytes as observed by confocal microscopy. Cells were fixed and stained with rhodamine–phalloidin for actin filaments (*A–C*), anti-β-catenin (*D*), or anti-E-cadherin antibodies for cell–cell contacts (*E and F*). *C* and *F* are projected *x–z* images of optical *z* sections taken using 0.5-μm steps. (*A*) Spread lower cells had numerous actin bundles and prominent circumferential bundles of actin filaments. (*B*) Upper spherical cell possessed blebs that were enriched for actin; however, these cells did not have prominent bundles of actin filaments. (*C*) Projected *z* series of the same cells shown in *A* demonstrates round shape of the upper cell (arrowhead) and spread cells attached to the substrate. (*D*) Lower spread cells formed continuous contacts among all cells of the monolayer, as evidenced by the well outlined rims identified by staining with anti-β-catenin antibodies. (*E*) Four upper spherical cells formed localized short contacts (arrows). (*F*) *x–z* projections of the same cells shown in *E* show the same cell–cell contacts between rounded cells (arrows) and contacts between lower cells of the monolayer. (Bar = 10 μm.)

cultures were treated with the selective inhibitor of Rho-kinase Y-27632 (20). After exposure to 15 μM Y-27632 for 1–2 h, the phenotypic changes of transfected cultures were fully reversed. Most spherical cells spread and become indistinguishable from other cells of the sheet. Thus, the observed changes in attached and round cell morphologies were most probably due to activated myosin II-contractile activity.

On many occasions, groups of cells from the upper tier would become dislodged from a main island of cells, whereupon the cell masses would either float within the culture media (Fig. 2*D* and Movie 2) and eventually resettle onto the substrate. After settling onto the substrate, the cell masses would undergo displacement along the substrate, often covering distances of 100 μm or greater. These displacements were not accompanied by formation of cytoplasmic outgrowths or by any other significant alterations of shape, an observation that suggests the movements were passive and possibly depend on microcurrents in the media. However, one cannot exclude the possibility that active bleb-dependent movements on the surface of the cells participated in the observed displacements (21).

The observation that dislodged and floating cell masses eventually settled on the substrate presents the possibility that this phenomenon may serve to seed the generation of another cell colony distant from the original population of cells. To confirm that detached floating cells remain alive and can form new colonies, cultures were grown to confluency, and the cells floating in the medium were collected, counted, and replated into fresh flasks. Floating cells accounted for 2–5% of total cell number in the flask of nearly confluent cells. Nearly 99% of these floating cells were alive, as confirmed by trypan blue staining. Equivalent preparation of nontransfected cultures did not have floating live cells in the culture medium. When the undiluted medium from transfected cultures with floating cells was plated into a new flask, ≈20–25% of the seeded cells were found loosely attached to the substrate after 3 h, often as small colonies averaging three cells. After 24–48 h, the total number of cells attached to the substrate did not increase, but most of these cells spread and started to divide, forming new colonies similar in morphology to those before reseeding. Thus, dislodging of cells from a colony followed by passive dispersal can serve as a means to recolonize on a distant cell-free substrate.

The apical surface of attached spread cells was covered with blebs, and the cytoplasm was full of actin stress fibers (Fig. 3*A*) that formed paxillin-containing focal cell–substrate contacts (not shown), providing further indication of increased cellular contractility. Substrate adherent cells had well developed circumferential bundles of actin filaments and adherens junctions, as determined by staining with β-catenin antibodies (Fig. 3*D*). The surface of spherical cells was completely covered with small blebs and enriched with a cortical layer of actin filaments (Fig. 3*B*). Surprisingly, spherical cells did not contain any detectable bundles of actin filaments or stress fibers (Fig. 3*B*). The spherical cells were linked with one another and with lower cells by short fragments of cadherin contacts (Fig. 3 *E* and *F*). Both spread and round cell types were filled with arrays of microtubules (not shown).

Analysis of cell dynamics in nontransfected IAR-2 cell cultures by time-lapse video microscopy determined that the cells did not exhibit significant movements except for lateral expansion of colonies after cell division. During cell division, control cells became rounded during mitosis, but after cytokinesis, the cells respread in 10–20 min and returned to their original spread shape (Fig. 4 *A* and *C*; also Movie 3, which is published as supporting information on the PNAS web site). In nearly all cases, cytokinesis occurred perpendicular to the substrate surface, as determined by the orientation of the mitotic spindle, which was parallel to the substrate (Fig. 5 *A* and *B*). Consequently, the daughter cells never lost contact with the substrate surface and were immediately incorporated into the epithelial sheet. In contrast, analysis of cell dynamics in transfected cultures showed that spherical cells originated from spread cells due to a change in the plane of the cleavage furrow from perpendicular to parallel to the substrate (Fig. 4 *B* and *C*). As

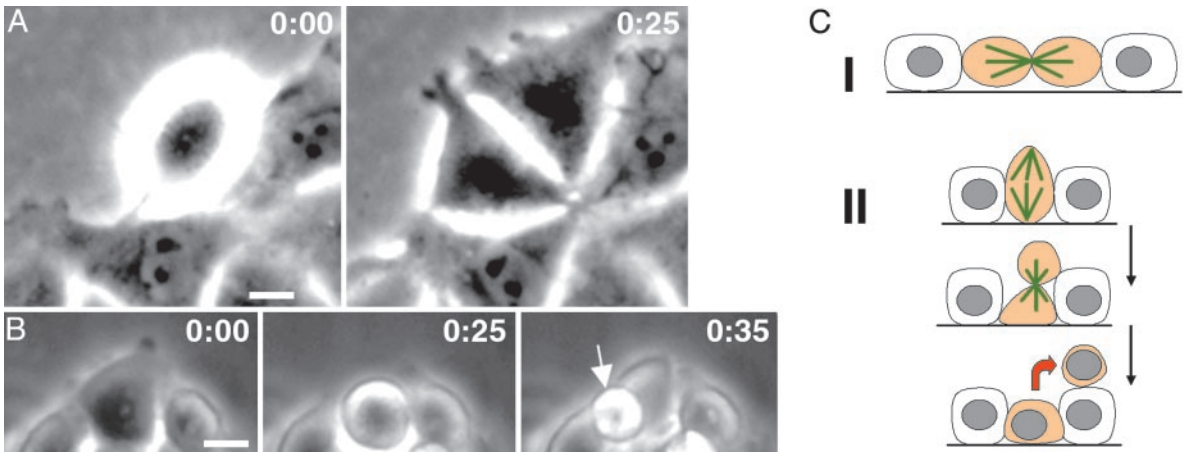


**Fig. 4.** Spherical cells in IAR-2 culture stably expressing constitutively active RhoA originate from altered cell division as observed by time lapse video microscopy. (*A*) Phase-contrast micrograph from a control culture showing conventional cell division occurring perpendicular to the plane of cell monolayer. After 25 min, the two initially rounded daughter respread back onto the substrate and remained attached to the monolayer. The full sequence is provided in Movie 3. (*B*) In transfected cells, cell division axis changed, often producing a cleavage plane that was parallel to the substrate. In this case, the upper rounded cell effectively budded from the monolayer, remained rounded, and was loosely attached to the lower cells. The entire sequence can be viewed in Movie 4. Time is shown in minutes. (Bar = 10 $\mu$m.) (*C*) Schematic of two different division orientations that lead to either cell continued cell substrate attachment (I) or production of budded spherical cells (II). Mitotic spindle is shown in green, mitotic cells are shown in orange, and cell transition is indicated by red arrow.

predicted, this reorientation occurred as a consequence of misorientation of the mitotic spindle leading to the long axis of the spindle being oriented perpendicular to the surface of the substrate (Fig. 5 *C* and *D*). During the course of this cell division, one daughter cell remained attached to the substrate and would respread, whereas the other daughter cell sat on the upper surface of its sister and remained rounded and loosely adherent (Fig. 4 *B* and *C*; Movie 4, which is published as supporting information on the PNAS web site). Misorientation of the division axis occurred with a significantly higher frequency in RhoA-overexpressing cells (26 per 51 mitoses, 52 ± 7%), as compared to their nontransfected cell relatives (4 per 50 mitoses, 0.8 ± 2%). Cell division-dependent formation of spherical floating cells was further confirmed by treatment with 0.5 mM hydroxyurea to block DNA synthesis and inhibit progression through the cell cycle. After 24–48 h of treatment, there were no detectable floating cells in cultures of constitutively active RhoA-expressing cells, thus confirming that formation of detached cells was associated with the cell division cycle.

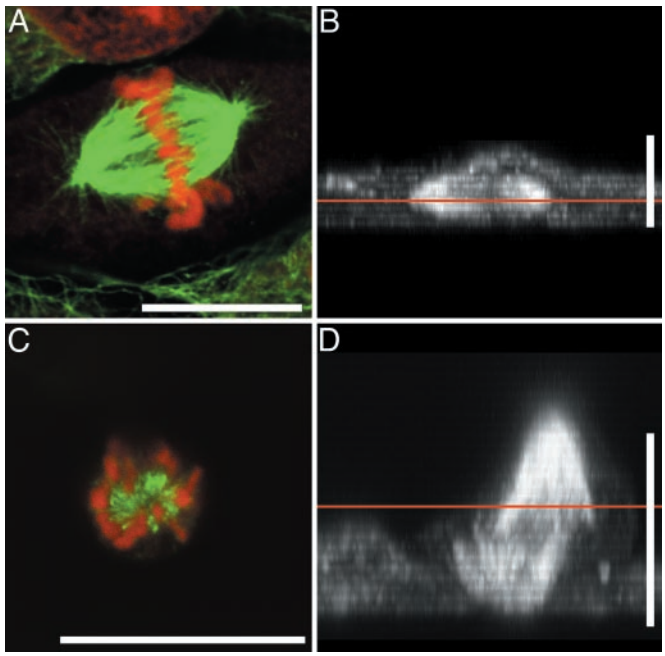


**Fig. 5.** Orientation of mitotic spindles in IAR-2 cells is changed upon stable expression of constitutively active RhoA. Cells were fixed and stained for $\alpha$-tubulin (green) with DM1$\alpha$ antibodies and for chromosomes (red) with propidium iodide. *x–z* projections of laser-scanning confocal images taken at 0.5-$\mu$m steps are shown in *B* and *D*. The straight red lines in *B* and *D* identify the plane of the images shown in *A* and *C*. (*A*) Confocal micrograph showing parallel orientation of the mitotic spindle relative to the substrate within a nontransfected cell. (*B*) *x–z* projection of *x–y* series of the cell shown in *A*. (*C*) Confocal micrograph of a mitotic spindle from a transfected cell showing a misoriented spindle whose axis lies perpendicular rather than parallel to the substrate (also see Movie 5, which is published as supporting information on the PNAS web site). (*D*) *x–z* projection of the cell from *C* showing the perpendicular or vertical orientation of the mitotic spindle. (Bar = 10 $\mu$m.)

## Discussion

**RhoA-Transfected Cells Demonstrate Increased Levels of Contractility.** Activation of RhoA leads to increased contractile activity through a Rho/Rho-kinase pathway, which leads to myosin II-mediated contraction (4, 22, 23). In our experiments, a constitutively active construct of RhoA, EGFP-RhoA Q63L, was stably transfected into IAR-2 epithelial cells producing a cell line that overexpressed active RhoA and mediated cellular effects via the Rho kinase pathway. Transfected cells possessed an increased density of actin stress fibers, exhibited a generalized contraction producing cells of smaller size, and last, the cells lost their ability to maintain monolayers in culture. Treatment with a selective inhibitor of Rho kinase reversed these changes, thus confirming that expression of the constitutively active construct was acting through a Rho/Rho-kinase pathway, which led to the observed contractility-dependent changes in phenotype.

**RhoA-Dependent Cell Detachment from Epithelial Monolayers Requires Mitotic Cells.** Expression of constitutively active RhoA in IAR-2 cells produced a profound change in the phenotype of IAR-2 cell cultures by producing two distinct populations of cells. One population of cells is spread and attached to the cell substrate, as observed with typical cell monolayers, whereas the second population consisted of spherical cells that were layered on top of the substrate adherent cells. Floating spherical cells represented

2–5% of the total cell count. What determines the entry into this fraction, and what is the relationship to RhoA activity? Our results indicate that active cell division is a prerequisite for creation of spherical cells, and direct video monitoring of transfected cultures showed that spherical cells appeared to "bud" from the surface of the monolayer at sites where lower cells in contact with the substrate were progressing through cell division. This association was confirmed by our experiments showing that when cell cycle progression was inhibited by treatment with hydroxyurea, round cells failed to form.

It is well known that in standard conditions when cells in culture undergo cell division, they are easily detached from the substrate by mechanical agitation. This property is used for synchronization of cells blocked in mitosis by colchicine (24). Facilitated detachment of cells from a substrate during normal cell division, in all probability, is due to the fact that entry into mitosis in most types of tissue culture cells is characterized by alterations of cell shape, specifically cell rounding. These shape alterations are accompanied and probably induced by disassembly of actin microfilament bundles, loss of stress fibers leading to diminished cell–substrate adhesion, partial disassembling of cell–cell contacts, and alterations in cortical actin filament dynamics and myosin II contractile activity. We suggest that overactivation of RhoA exacerbates these alterations that in turn drive nonphysiological breakage of cell–cell and cell–substrate contacts and enhance the levels of myosin II contraction within the cell cortex. Consequently, the process of cell division in cells having overstimulated RhoA activity initiated related activities that prevented cells from maintaining normal physiological contact with their substrate and neighbors.

One of the most surprising findings in our experiments was that stimulation of Rho induced alterations in the orientation of the mitotic spindle relative to the substrate and the epithelial sheet (see Fig. 4*C*). The exact mechanism that regulates proper orientation of the mitotic spindle in normal monolayer during cell division remains speculative; however, there may exist "positional cues" directed by the presence of the cell–cell contacts (25, 26). Presently, there is a substantial body of evidence indicating that the interaction of astral microtubules of the mitotic spindle with the cortical actin cytoskeleton is essential for proper orientation and positioning of the mitotic spindle and subsequent cleavage furrow (27). One possible explanation of the effect of RhoA expression on orientation of mitosis is suggested by the recent work of Rosenblatt *et al.* (28), who showed that myosin II-dependent cortical contraction controls the movement of cell cortex and of associated astral microtubules of the mitotic spindle. We suggest that alteration of the activity of myosin II within the cortex of the cell by RhoA overexpression may induce abnormalities of mitotic spindle orientation, eventually facilitating the detachment of daughter cells from an epithelial sheet.

**Alterations Induced by Rho Overactivation in Cultures of Epithelial Cells May Be Similar to Molecular Alterations Responsible for Cancer Dissemination *in Vivo*.** The phenotypic activity of IAR-2 epithelial cells expressing constitutively active RhoA may serve as a useful *in vitro* experimental model for understanding dissemination of neoplastic cells *in vivo*. The data presented in this work propose that active cell detachment from the primary mass of cell (epithelial sheet, tumor) may be followed by rapid largely passive movements through the media/circulation, leading to new colonization at a distant site. This type of cell dissemination is mechanistically different from the commonly accepted pathway of cancer invasion predicated on epithelial–mesenchymal transformation of neoplastic cells and their subsequent active translocation on a substrate to a new colonization site (29, 30). Recently, Sahai and Marshall (21) identified two modes of motility in mouse tumor lines growing in 3D matrices: elongated cell motility associated with Rac-dependent protrusions and rounded bleb-dependent motility associated with increased Rho and Rho-kinase function. Overexpression of constitutively active RhoA may be sufficient to induce the formation of this second cell type, whereby these cells may rapidly disperse by floating and forming distant metastatic colonies, whereas the cells of the first elongated type may be responsible for crawling invasion. Thus, various forms of cancer dissemination may be associated with different molecular alterations of Rho family members and possibly may require different approaches to treatment. Last, it is worth noting that our experiments identified a previously unappreciated correlation between unregulated proliferation of cancer cells and their dissemination, namely an increased frequency of cell division, that may promote cell detachment and subsequent dispersal.

We thank Dr. G. Bokoch (The Scripps Research Institute, La Jolla, CA) for providing a plasmid. This work was supported by a Russian Foundation of Basic Investigation grant and a Ludwig Foundation grant (to J.M.V.), by a gracious gift from an anonymous donor to the Research Exchange Program at Rutgers–Newark, and by a Johnson & Johnson Discovery Award (to E.M.B.).

1. Etienne-Manneville, S. & Hall, A. (2002) *Nature* **420,** 629–635.
2. Bishop, A. L. & Hall, A. (2000) *Biochem. J.* **348,** 241–255.
3. Omelchenko, T., Vasiliev, J. M., Gelfand, I. M., Feder, H. H. & Bonder, E. M. (2002) *Proc. Natl. Acad. Sci. USA* **99,** 10452–10457.
4. Omelchenko, T., Vasiliev, J. M., Gelfand, I. M., Feder, H. H. & Bonder, E. M. (2003) *Proc. Natl. Acad. Sci. USA* **100,** 10788–10793.
5. Lozano, E., Betson, M. & Braga, V. M. (2003) *BioEssays* **25,** 452–463.
6. Sahai, E. & Marshall, C. J. (2002) *Nat. Rev. Cancer* **2,** 133–142.
7. Horiuchi, A., Imai, T., Wang, C., Ohira, S., Feng, Y., Nikaido, T. & Konishi, I. (2003) *Lab. Invest.* **83,** 861–870.
8. Pan, Y., Bi, F., Liu, N., Xue, Y., Yao, X., Zheng, Y. & Fan, D. (2004) *Biochem. Biophys. Res. Commun.* **315,** 686–691.
9. Ikoma, T., Takahashi, T., Nagano, S., Li, Y. M., Ohno, Y., Ando, K., Fujiwara, T., Fujiwara, H. & Kosai, K. (2004) *Clin. Cancer Res.* **10,** 1192–1200.
10. Clark, E. A., Golub, T. R., Lander, E. S. & Hynes, R. O. (2000) *Nature* **406,** 532–535.
11. Kamai, T., Tsujii, T., Arai, K., Takagi, K., Asami, H., Ito, Y. & Oshima, H. (2003) *Clin. Cancer Res.* **9,** 2632–2641.
12. Kleer, C. G., van Golen, K. L., Zhang, Y., Wu, Z. F., Rubin, M. A. & Merajver, S. D. (2002) *Am. J. Pathol.* **160,** 579–584.
13. Shikada, Y., Yoshino, I., Okamoto, T., Fukuyama, S., Kameyama, T. & Maehara, Y. (2003) *Clin. Cancer Res.* **9,** 5282–5286.
14. Subauste, M. C., Von Herrath, M., Benard, V., Chamberlain, C. E., Chuang, T. H., Chu, K., Bokoch, G. M. & Hahn, K. M. (2000) *J. Biol. Chem.* **275,** 9725–9733.
15. Montesano, R., Saint Vincent, L., Drevon, C. & Tomatis, L. (1975) *Int. J. Cancer* **16,** 550–558.
16. Ren, X. D., Kiosses, W. B. & Schwartz, M. A. (1999) *EMBO J.* **18,** 578–585.
17. Benard, V. & Bokoch, G. M. (2002) *Methods Enzymol.* **345,** 349–359.
18. Omelchenko, T., Fetisova, E., Ivanova, O., Bonder, E. M., Feder, H., Vasiliev, J. M. & Gelfand, I. M. (2001) *Proc. Natl. Acad. Sci. USA* **98,** 8632–8637.
19. Riento, K. & Ridley, A. J. (2003) *Nat. Rev. Mol. Cell. Biol.* **4,** 446–456.
20. Uehata, M., Ishizaki, T., Satoh, H., Ono, T., Kawahara, T., Morishita, T., Tamakawa, H., Yamagami, K., Inui, J., Maekawa, M. & Narumiya, S. (1997) *Nature* **389,** 990–994.
21. Sahai, E. & Marshall, C. J. (2003) *Nat. Cell Biol.* **5,** 711–719.
22. Hall, A. (1998) *Science* **279,** 509–514.
23. Arthur, W. T. & Burridge, K. (2001) *Mol. Biol. Cell* **12,** 2711–2720.
24. Merrill, G. F. (1998) *Methods Cell Biol.* **57,** 229–249.
25. Ahringer, J. (2003) *Curr. Opin. Cell. Biol.* **15,** 73–81.
26. Le Borgne, R., Bellaiche, Y. & Schweisguth, F. (2002) *Curr. Biol.* **12,** 95–104.
27. Wang, Y. L. (2001) *Cell Struct. Funct.* **26,** 633–638.
28. Rosenblatt, J., Cramer, L. P., Baum, B. & McGee, K. M. (2004) *Cell* **117,** 361–372.
29. Thiery, J. P. (2002) *Nat. Rev. Cancer* **2,** 442–454.
30. Friedl, P. & Wolf, K. (2003) *Nat. Rev. Cancer* **3,** 362–374.